RSC Advances

PAPER

View Article Online
View Journal | View Issue

Cite this: *RSC Adv.*, 2025, **15**, 35407

The effect of platinum nanoparticles on the physicochemical properties of daunorubicin

Marcin Zakrzewski,[a] Patrycja Bełdzińska,[a] Felicja Gajdowska,[bc] Grzegorz Gołuński,[a] Karolina Gackowska,[d] Justyna Strankowska,[e] Marzena Jamrógiewicz,[f] Dariusz Wyrzykowski,[g] Katarzyna Grzyb,[h] Danuta Gutowska-Owsiak,[c] Anna Synak,[e] Piotr Bojarski[e] and Jacek Piosik *[a]

Cancer is a difficult disease to cure due to its diversity and complexity. Despite novel therapeutic approaches having been proposed in recent years, chemotherapy remains one of the most common treatment regimens to this day. Unfortunately, its anticancer effects are often quelled by the lack of selectivity; hence alteration of the activity of already existing drugs by combining them with potential modulators *e.g.* metallic nanoparticles has been proposed as a possible strategy to overcome this problem. Herein, we verified if platinum nanoparticles (PtNPs) of various sizes interact with daunorubicin (DAU), a chemotherapeutic agent used for the treatment of leukaemia. Utilizing DLS and NTA we observed nanoparticle aggregation upon addition of increasing concentrations of DAU. Furthermore, we noticed that PtNPs quench DAU's fluorescence, suggesting their direct interaction. Next, we used FTIR and NIR spectroscopies and registered significant changes in the obtained spectra in the presence of PtNPs. The ITC and DSC analyses showed that all tested sizes of PtNPs interact with DAU in an endothermic manner, with the enthalpy change between 0.47 and 4.36 kcal mol^{-1}. The release analysis employing the dialysis bag method evidenced that PtNPs influence DAU's diffusion kinetics, decreasing its release from 100% (when alone) to *ca.* 70% when combined with PtNPs. All tested sizes of PtNPs reduce DAU's mutagenicity towards *S.enterica* serovar Typhimurium TA98 strain, however, no significant influence on DAU's cytotoxicity was observed on neither MelJuSo nor HaCaT eukaryotic cell lines. Overall, these results indicate that PtNPs may affect DAU's biological activity and warrant further biological studies.

Received 23rd April 2025
Accepted 16th September 2025

DOI: 10.1039/d5ra02827b

rsc.li/rsc-advances

1 Introduction

Cancer prevalence is increasing worldwide due to the aging populations and lifestyle changes, and is among the three leading causes of death in the age group 30–60 years old in almost all countries.[1] By 2050, the gross number of all new cases diagnosed annually is expected to increase from 20 to approximately 35 million.[1] Currently diverse treatment regimens are employed, including both surgical intervention and pharmacotherapy. However, while the number of approved anti-cancer agents has increased almost every year over the course of the past decade, according to the 2021 FDA report the percentage of new therapeutics with novel mechanisms of action within a given type of cancer has declined.[2] Despite numerous advancements in the field (incl. immunotherapy), chemotherapy remains the main mode of treatment, especially in newly diagnosed patients.[3] Regardless of how effective it may be, it is not indifferent to the healthy cells, contributing to major side effects, such as cardiotoxicity, neurotoxicity, or myelosuppression, thus making the therapy unsustainable in the long run.[4] A potential solution to this problem is the

[a]*Laboratory of Biophysics, Intercollegiate Faculty of Biotechnology UG and MUG, University of Gdańsk, 80-307, Gdańsk, Poland. E-mail: marcin.zakrzewski@phdstud.ug.edu.pl; patrycja.beldzinska@phdstud.ug.edu.pl; grzegorz.golunski@ug.edu.pl; jacek.piosik@ug.edu.pl*

[b]*Laboratory of Experimental and Translational Allergology and Pneumonology, Medical University of Gdańsk, 80-210, Gdańsk, Poland. E-mail: felicja.gajdowska@gmail.com*

[c]*Laboratory of Experimental and Translational Immunology, Intercollegiate Faculty of Biotechnology UG and MUG, University of Gdańsk, 80-307, Gdańsk, Poland. E-mail: danuta.gutowska-owsiak@ug.edu.pl*

[d]*Laboratory of Recombinant Vaccines, Intercollegiate Faculty of Biotechnology UG and MUG, University of Gdańsk, 80-307, Gdańsk, Poland. E-mail: karolina.gackowska@phdstud.ug.edu.pl*

[e]*Division of Biomaterials and Medical Physics, Faculty of Mathematics, Physics and Informatics, University of Gdańsk, 80-308, Gdańsk, Poland. E-mail: justyna.strankowska@ug.edu.pl; anna.synak@ug.edu.pl; piotr.bojarski@ug.edu.pl*

[f]*Department of Physical Chemistry, Faculty of Pharmacy, Medical University of Gdańsk, 80-416, Gdańsk, Poland. E-mail: marzena.jamrogiewicz@gumed.edu.pl*

[g]*Department of General and Inorganic Chemistry, Faculty of Chemistry, University of Gdańsk, 80-308, Gdańsk, Poland. E-mail: dariusz.wyrzykowski@ug.edu.pl*

[h]*Laboratory of Virus Molecular Biology, Intercollegiate Faculty of Biotechnology UG and MUG, University of Gdańsk, 80-307, Gdańsk, Poland. E-mail: katarzyna.grzyb@ug.edu.pl*

incorporation of nanoparticles into the drug formulation, creating Nanoparticle Drug Therapy (NDT). This approach aims to enhance the efficacy, selectivity, and bioavailability of the drug within the tumour.

Nanoparticles (NPs) have received interest from the scientific community since the last century.[5] In general, they can be characterized as structures ranging from 1 to 100 nm in size and can be divided into three groups, *i.e.*, inorganic, organic, and carbon-based nanoparticles. Due to the variety of size, shape, composition, optical properties, and, additionally, possible surface functionalization,[5–7] NPs exhibit a broad spectrum of features. As a consequence, they were found to be important in numerous scientific and clinical applications, including medicine, as antibacterial substances, biosensors, or anticancer agents, acting either directly or as drug carriers.[6] Among metallic nanoparticles, platinum nanoparticles (PtNPs) have gained interest in recent years. They have been shown to be cytotoxic against various cancer cell lines,[8–11] mainly through the production of reactive oxygen species (ROS) and causing cell damage to those lines, but with no significant cytotoxic effects to the healthy cells.[10,12,13] PtNPs have also been applied as nanocarriers, leading to the possibility of lowering the dose of the drug whilst maintaining its efficacy.[14,15] Furthermore, since the pH of tumour cells is known to be lower than that of healthy cells,[16,17] there is an additional opportunity through combining the drug with nanoparticles allowing for its increased selectivity through a pH dependent release.[18,19]

Daunorubicin (DAU), an anthracycline antibiotic discovered in mid-60's, was soon recognized as a potent anticancer agent, especially in the treatment of lymphoblastic and myeloblastic leukaemia. The three main modes of its activity are the production of ROS, intercalation to DNA, and inhibition of topoisomerase II activity, ultimately leading to cell death.[20,21] Unfortunately, DAU is also associated with significant side effects, mainly cardiotoxicity and bone marrow suppression.[20] Cardiotoxic effects may persist for up to five years after treatment.[22] Additional adverse effects include therapy-related tumorigenesis and gonadotoxicity.[23]

Unfortunately, the current knowledge regarding the possible influence of nanoparticles on cancer chemotherapy is still limited and requires detailed studies. Bearing in mind the numerous properties of metallic nanoparticles, we decided to study whether platinum nanoparticles of different sizes interact with daunorubicin and if so, what are the *in vitro* biological implications of these interactions. To do so, we employed various physicochemical methods, as well as biological assays.

2 Experimental

2.1 Materials

Platinum nanoparticles (PtNPs) at concentrations 0.05 mg mL^{-1} and 1 mg mL^{-1} were obtained from nanoComposix (San Diego, California, USA). The nanoparticles were suspended in 2 mM sodium citrate for 5, 30 and 50 nm PtNPs and in 4 mM sodium citrate for 70 nm PtNPs. Daunorubicin hydrochloride (DAU) was obtained from Sigma-Aldrich (Saint Louis, Missouri, USA). The stock solutions were prepared by dissolving DAU in water and the desired concentration was validated *via* spectroscopic methods with the molar extinction coefficient of $\varepsilon_{545} = 5.4 \times 10^3\ M^{-1}\ cm^{-1}$. The phosphate-citrate buffers with pH 5.4, 6.4 and 7.4, were prepared according to the buffers for pH and metal ion control[24] protocol, utilizing citric acid monohydrate from VWR Chemicals (Radnor, Pennsylvania, USA) and sodium phosphate from Sigma-Aldrich (Saint Louis, Missouri, USA). The chemicals were dispersed in deionized water and their pH was validated using pH-meter from Mettler Toledo (Columbus, Ohio, USA). The sodium citrate tribasic dihydrate was obtained from Sigma-Aldrich (Saint Louis, Missouri, USA). The Spectra/Por 7 dialysis tubing of 10 000 MWCO were bought from Repligen (Waltham, Massachusetts, USA).

Salmonella enterica serovar Typhimurium TA98 strain was purchased from Xenometrics AG (Allschwil, Switzerland). Nutrient Agar, Nutrient Broth and Biological Agar media were purchased from BioMaxima S.A. (Gdansk, Poland). Histidine, biotin, and ampicillin were acquired from Sigma Aldrich Chemical Company (St. Louis, Missouri, USA). Human keratinocyte cell line (HaCaT) and human melanoma cell line (Mel-JuSo) were obtained from the Department of Microbiology, Tumor and Cell Biology, Karolinska Institute (Stockholm, Sweden) and the Department of Medicinal Microbiology, Leiden University Medical Center (Leiden, The Netherlands), respectively. Dulbecco's modified Eagle's medium (DMEM), Roswell Park Memorial Institute (RPMI) 1640 Medium, and 10% fetal bovine serum (FBS), 4 mM L-glutamine, glucose and antibiotic-antimycotic solution were purchased from ThermoFisher Scientific (Waltham, Massachusetts, USA).

2.2 Dynamic light scattering (DLS)

The hydrodynamic diameter of the PtNPs and the change in registered sizes upon the addition of DAU were evaluated in polystyrene cuvettes at 25 °C utilizing Zetasizer Nano S from Malvern Panalytical (Malvern, Great Britain). The initial concentration of PtNPs was 2.38 μg mL^{-1}, the concentration range of DAU was 4.2–42 μM. All of the measurements were done in triplicates, each consisting of six measurements, 10 seconds per measurement. The data was processed by Zetasizer software.

2.3 Nanoparticle tracking analysis (NTA)

To visualize how platinum nanoparticles interact with daunorubicin in aqueous environment and to further evaluate their size alone and in combination with the drug, we performed a nanoparticle tracking analysis using Nanosight NS300 from Malvern Panalytical (Malvern, Great Britain), with a sCMOS camera and a blue 488 nm laser. PtNPs, at concentration 0.0025 mg mL^{-1}, were added to the cell, and measured in a stationary manner, with 5 recorded videos, 1 minute each. Next, after rinsing the cell with deionized water, a solution of 0.0025 mg mL^{-1} of PtNPs and 21.7 μM DAU was added to the measurement cell, and recorded as previously described. Due to the limitations in the apparatus' range of measurements, 5 nm PtNPs had to be excluded from the procedure. The nanoparticles were diluted in deionized water.

2.4 Fluorescence spectroscopy

The fluorescence measurements were performed in quartz cuvettes at temperature 25 ± 0.1 °C using Jasco FP-8500 (Jasco, Easton, Maryland, USA) with a Peltier thermostat. In each sample the initial concentration of DAU was 34.7 μM followed by titration with PtNPs in the concentration range 0–10.62 mg mL^{-1}. All the measurements were performed in 2 mM sodium citrate for 5, 30 and 50 nm PtNPs and in 4 mM sodium citrate for 70 nm PtNPs. For the negative control the DAU was titrated with analogous volumes of appropriate sodium citrate solution. The excitation was set at 480 nm, and the emission was registered withing 400–800 nm range.

2.5 Fourier transform infrared spectroscopy (FTIR) and near infrared spectroscopy (NIR)

FTIR and NIR spectra of complexes formed between daunorubicin and platinum nanoparticles were recorded on Jasco-4700 instrument (IR: 4000–400 cm^{-1} NIR: 8200–4000 cm^{-1}) with 32 scans, 4 cm^{-1} resolution; (Jasco Company, Tokyo, Japan). All prepared samples were lyophilized prior to the procedure. NIR Transmission technique was applied using dry salt KBr and dry samples of DAU, PtNPs, and sodium citrate obtained in the process of lyophilization. The materials were compressed with potassium bromide to form a disc. All spectra were recorded as a background and analysis of spectra was performed using Spectra Analysis software (Jasco Company, Tokyo, Japan).

2.6 Isothermal titration calorimetry (ITC)

Isothermal titration calorimetry measurements were performed at 25 °C on AutoITC isothermal titration calorimeter (MicroCal Inc. GE Healthcare, Northampton, Massachusetts, USA). The volumes of the sample and reference cells were 1.4491 mL. The experiment consisted of 15 injections of 10.02 μL with a 2 μL for the first injection only of DAU solution (concentration range 0.002–0.029 mM) into the sample cell containing PtNPs (initial concentration 0.05 mg mL^{-1}). Background titrations were performed by injecting DAU into the appropriate sodium citrate solution and appropriate sodium citrate solution to PtNPs. The results of the background titrations were subtracted from each experimental result to account for the heat of dilution. Using linear regression, we calculated the exact values of enthalpy. Each injection lasted 20 s. To reach a homogenous mixing in the cell, the stirrer speed was kept constant at 300 rpm.

2.7 Differential scanning calorimetry (DSC)

The thermal behaviour of the samples was measured by Differential Scanning Calorimetry (DSC), STAR-1 System, Mettler Toledo (Greifensee, Switzerland), which was calibrated with indium. The analysis was carried out in aluminum crucibles 40 μL at the temperature range from 20 °C to 300 °C. For performing the DSC, 1–5 mg of the appropriate sample was weighed. DSC curves were recorded and analysed by the STAR-1 System (Mettler Toledo, Greifensee, Switzerland) combined with the intercooler system. Samples were heated at the heating rate of 10 °C min^{-1} and a nitrogen flow rate 60 mL min^{-1}. All tests were standardized to each sample size.

2.8 Release analysis using dialysis bag technique

The release analysis of daunorubicin from PtNPs-DAU aggregates was conducted using dialysis bags from Repligen (Waltham, Massachusetts, USA) with a Molecular Weight Cut Off (MWCO) of 10 kDa, at room temperature. Prior to the procedure, a DAU-PtNPs mixture was prepared; 1800 μL of PtNPs at a concentration of 0.05 mg mL^{-1} and 200 μL of DAU at a concentration of 2 mg mL^{-1} were added to an Eppendorf tube and left to mix for 24 hours at room temperature. A beaker with a 50 mL capacity was filled with 28 mL of citrate-phosphate buffer at the desired pH, and a magnetic stirrer was placed inside. A dialysis bag of appropriate length was prepared, 2 mL of the incubated mixture was added and the membrane was closed tightly. 2 mL of citrate-phosphate buffer at the desired pH was added to a quartz cuvette with an optical path length of 1 cm, and absorption was measured in a spectrophotometer as a baseline. The prepared dialysis bag was placed in the beaker with the buffer, and at desired intervals 2 mL of the solution was taken from the beaker and placed in a new measurement cuvette with the same parameters as above for absorption measurements. The solution from each timepoint was returned to the beaker.

The concentration of released daunorubicin was calculated using the molar extinction coefficient of DAU which was spectrophotometrically obtained prior to the experimental procedure. The absorption results of each concentration were averaged and then converted to concentration using the Lambert–Beer law: $A = \varepsilon \times c \times l$, where A is absorption, ε is the molar extinction coefficient ($\varepsilon_{545} = 5.4 \times 10^3\ M^{-1}\ cm^{-1}$), c is the concentration of the substance (mol L^{-1}), and l is the optical path length (cm). The analysis of the release process was performed based on two mathematical models, Korsmeyer–Peppas and Hopfenberg, to the experimental release curves. The models are explained in detail in the SI.

2.9 Ames mutagenicity assay

The influence of PtNPs on the mutagenic activity of DAU was assessed using the Ames mutagenicity plate assay with *Salmonella enterica* serovar Typhimurium TA98 strain, according to the procedure described by Woziwodzka *et al.*[25] A mixture containing 100 μL of the overnight bacteria culture, 50 μL of 3% NaCl, and 100 μL of the tested solution (or sterile distilled water as a negative control) was incubated for 4 h in darkness at 37 °C and 220 rpm. Afterwards, the mixture was centrifuged at 11 840 g, the bacterial pellet was washed with 0.75% NaCl, and resuspended in 300 μL of 0.75% NaCl solution containing 0.1 μM histidine and 0.1 μM biotin. The bacterial suspension was spread on a glucose minimal agar plate and incubated at 37 °C in darkness. After 48 h incubation, the number of revertant colonies per plate was calculated. All experiments were performed in triplicate.

2.10 Cell culture and cytotoxicity assay

The HaCaT cell line was cultivated in DMEM containing 4500 mg L^{-1} glucose, supplemented with 10% fetal bovine serum, 4 mM L-glutamine, 100 units mL^{-1} penicillin, 100 mg mL^{-1} streptomycin, and 0.25 μg mL^{-1} amphotericin B. The MelJuSo cell line was cultured in RPMI 1640 Medium supplemented with 10% fetal bovine serum, 4 mM L-glutamine, 100 units mL^{-1} penicillin, 100 mg mL^{-1} streptomycin, and 0.25 μg mL^{-1} amphotericin B. Both cell lines were maintained in a humidified atmosphere containing 5% CO_2 at 37 °C.

HaCaT and MelJuSo cells were seeded on a 96-well plate (2×10^4 cells/well) and incubated overnight in humidified atmosphere at 37 °C and with 5% CO_2. Next, the cells were washed thrice with appropriate medium devoid of FBS. Subsequently, PtNPs alone, at concentrations 0.2 and 1 μg per well or with 25 μM DAU, were added to cell cultures (90 μL per well), each sample in three replicates and incubated for 20 h. After that, 10 μL of alamarBlue (BioRad, Hercules, California, USA) was added to each well, and the plates were further incubated for 4 h in conditions described above. The absorbance was measured at 570 nm and 600 nm, and the percentage of alamarBlue reduction was calculated as a difference between treated and untreated cells, according to the protocol provided by the manufacturer, using the data gathered from 570 and 600 nm scans.

2.11 Computational and statistical analysis

All of the graphs were prepared in SigmaPlot 14.5 from Systat Software Inc (San Jose, California, USA). The release modelling was prepared using Origin from OriginLab (Northamtpon, Massachusetts, USA). Statistical analysis was conducted using Statistica 14.0 (TIBCO Software Inc., Palo Alto, California, USA) software. For the Ames mutagenicity test and release analysis, one-way variance analysis (ANOVA) followed by the post-hoc Tukey's HSD test was applied. For the cytotoxicity assay U-Mann Whitney test was used. The significance level for all the analyses was established at $\alpha = 0.05$.

3 Results and discussion

3.1 DAU-PtNPs aggregation

Dynamic light scattering (DLS) has proven to be a reliable method for particle size analysis, however, the results available in the literature vary when it comes to the interactions between

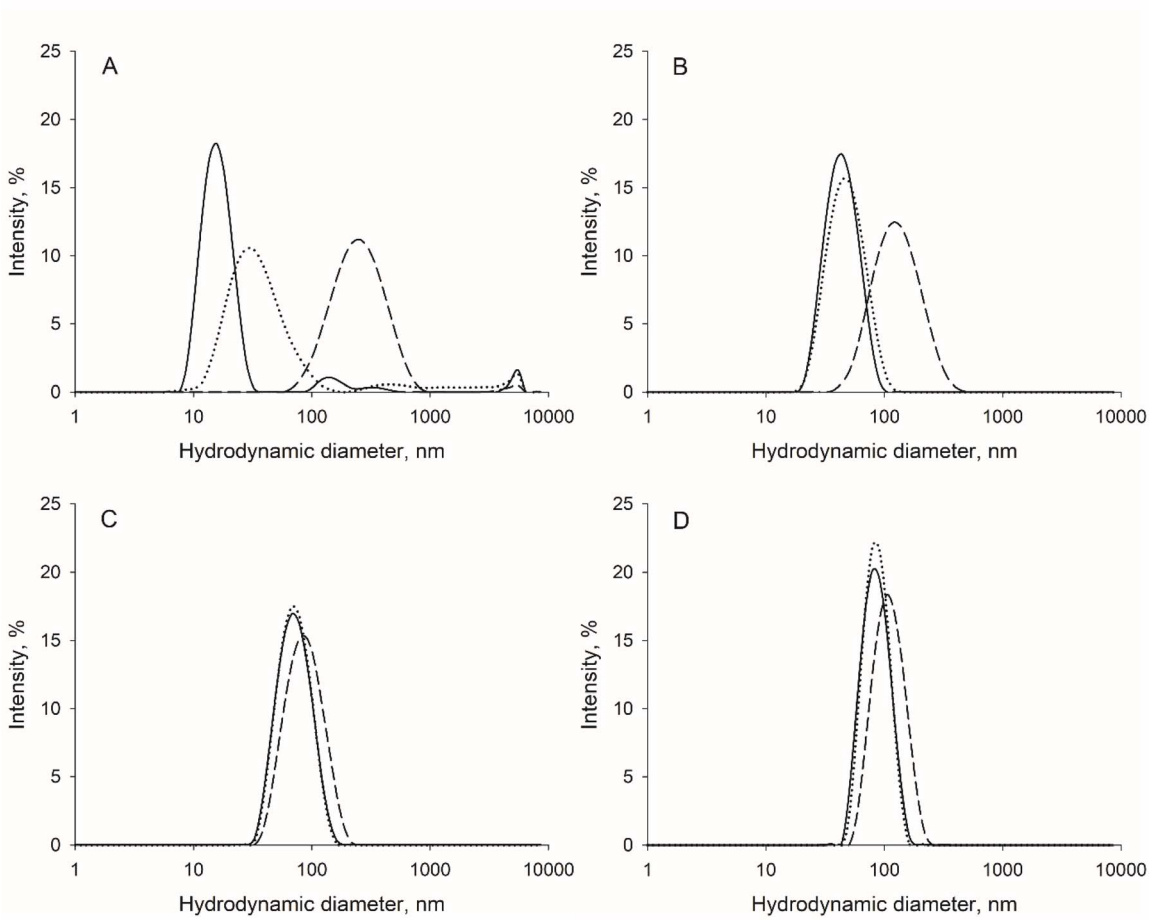

Fig. 1 Hydrodynamic diameter distribution of platinum nanoparticles (PtNPs) alone and in combination with daunorubicin (DAU). (A) 5 nm PtNPs, (B) 30 nm PtNPs, (C) 50 nm PtNPs, (D) 70 nm PtNPs. Solid line – nanoparticles alone, dotted line – nanoparticles with 4.2 μM DAU, dashed line – nanoparticles with 42 μM DAU; PtNPs initial concentration 2.5 μg mL^{-1}.

nanoparticles (NPs) and chemicals. In our previous study, we observed the formation of heteroaggregates between doxorubicin (DOX) and 5 nm and 50 nm silver nanoparticles in a dose-dependent manner,[26] as well as aggregation of fullerene C_{60} with DOX[27] and heteroaggregation between platinum nanoparticles (PtNPs) and ICR-191,[10] all of them resulting in a change of biological activity of the analysed active substance. On the other hand, cisplatin, did not promote significant change in registered diameter for 5 nm and 50 nm PtNPs based on DLS data, yet the remaining results suggested their interaction.[11] Herein, we observed a shift towards greater sizes upon the addition of daunorubicin (DAU) to PtNPs in all tested samples (Fig. 1). 5 nm PtNPs presented a polydisperse distribution, with three distinct peaks of 16.2, 201 and 5199 nm (Table 1). The addition of DAU resulted in a shift towards greater hydrodynamic diameters; *i.e.*, 36.9, 437.1 and 5165 nm for 4.2 μM DAU, and to 273.9 and 4825 nm for 42 μM DAU. In the case of 30, 50 and 70 nm PtNPs the nanoparticles alone were monodisperse and the change in registered size was mainly visible with the addition of 42 μM DAU, which was calculated as a 3.06-fold, 1.22-fold and 1.3-fold increase in the hydrodynamic diameter, respectively. Overall, the acquired results suggest formation of heteroaggregates between PtNPs and DAU and, possibly, homoaggregates of PtNPs alone. It is worth noting that the polydispersity index (PdI) remained below 0.3 in all the experiments, indicating the reliability of the obtained results.[28]

Among the available methods for particle diameter and distribution examination, nanoparticle tracking analysis (NTA) has significantly developed throughout the last two decades. Even though both DLS and NTA focus on determining the size of registered particles, the advantage of using the latter is that it can provide an approximate concentration of the measured particles, offering valuable insight into the kinetics of possible interactions within the sample.[29] The average size of 30 nm PtNPs was recorded as 38.8 nm by the NTA analysis, with a concentration of approximately 1×10^9 particles per mL. Upon the addition of DAU, the average diameter changed to 189.3 nm, with the concentration decreasing to 9.9×10^7 particles per mL, which suggests increased NPs aggregation. For 50 nm PtNPs, the addition of daunorubicin shifted the diameter from 61.3 nm to 125.8 nm, simultaneously lowering the concentration from 5.5×10^8 particles per mL to 1.1×10^8 particles per mL. In the case of 70 nm PtNPs, the mean size changed from 86.5 nm to 160.2 nm, with the concentration dropping down from 2.2×10^8 particles per mL to 6.8×10^7 particles per mL (Table 2).

A representative video of 30 nm platinum nanoparticles alone and in combination with daunorubicin is available in the supplementary materials (SI Video 1 and SI Video 2).

Table 1 Mean size of platinum nanoparticles (PtNPs) alone and in combination with daunorubicin (DAU). PdI – polydispersity index, SD – standard deviation

Sample	PdI ± SD	Mean size, nm ± SD	Area, % ± SD
5 nm PtNPs	0.26 ± 0.06	16.2 ± 0.4	91.8 ± 5.9
		201 ± 11.3	5.6 ± 4.8
		5199 ± 3001.6	2.6 ± 4.6
5 nm PtNPs + 4.2 μM DAU	0.26 ± 0.09	36.9 ± 9.2	90.1 ± 4.3
		437.1 ± 252.4	2.8 ± 4.9
		3597 ± 1812.17	7.1 ± 3.5
5 nm PtNPs + 42 μM DAU	0.2 ± 0.04	273.9 ± 55.4	98.8 ± 2.1
		4825 ± 2785.7	1.2 ± 2.1
30 nm PtNPs	0.09 ± 0.01	45.4 ± 0.9	100
30 nm PtNPs + 4.2 μM DAU	0.12 ± 0.01	49.8 ± 0.8	100
30 nm PtNPs + 42 μM DAU	0.15 ± 0.01	138.8 ± 28.2	100
50 nm PtNPs	0.09 ± 0.02	74.1 ± 1.9	100
50 nm PtNPs + 4.2 μM DAU	0.08 ± 0.01	74 ± 1.9	100
50 nm PtNPs + 42 μM DAU	0.11 ± 0.02	90.7 ± 0.3	100
70 nm PtNPs	0.08 ± 0.03	87.2 ± 1.1	100
70 nm PtNPs + 4.2 μM DAU	0.04 ± 0.01	87.6 ± 0.8	100
70 nm PtNPs + 42 μM DAU	0.08 ± 0.01	113.2 ± 5.3	100

Table 2 Mean size, mode, and concentration of platinum nanoparticles (PtNPs) alone and in combination with daunorubicin (DAU) obtained from NTA. SD – standard deviation

Sample	Mean size, nm ± SD	Mode, nm ± SD	Concentration, particles/mL ± SD
30 nm PtNPs	38.8 ± 1.4	29.8 ± 0.7	$1 \times 10^9 \pm 3.3 \times 10^7$
30 nm PtNPs + 21.7 μM DAU	189.3 ± 9.4	124.4 ± 17	$9.9 \times 10^7 \pm 1.2 \times 10^7$
50 nm PtNPs	61.3 ± 0.5	59.2 ± 0.5	$5.5 \times 10^8 \pm 2.8 \times 10^7$
50 nm PtNPs + 21.7 μM DAU	125.8 ± 6.5	86.7 ± 5.5	$1.1 \times 10^8 \pm 1.5 \times 10^7$
70 nm PtNPs	86.5 ± 1.1	73.8 ± 0.8	$2.2 \times 10^8 \pm 1.2 \times 10^7$
70 nm PtNPs + 21.7 μM DAU	160.2 ± 7.1	110 ± 8.4	$6.8 \times 10^7 \pm 6 \times 10^6$

Interestingly, the observed values were greater compared to the DLS results, however, the dissimilarity is possibly caused by different way of obtaining and processing of the data between these two methods. As mentioned above, particles concentration lowered after the DAU addition within all tested diameters of PtNPs, which was also visible as a change in the size and particle movement trajectories in the recorded movies, thus once more suggesting that DAU promotes the aggregation of PtNPs.

3.2 PtNPs influence on DAU spectra

Daunorubicin has two aromatic rings in its structure, therefore we used fluorescence spectroscopy to further confirm if the platinum nanoparticles interact with daunorubicin. Upon titrating DAU with increasing volumes of PtNPs (solid lines and triangles), the fluorescence significantly quenched compared to the negative control (solid lines and dots), where the drug was titrated with appropriate sodium citrate buffer (Fig. 2). The observed pattern was consistent and confirmed through additional independent experiments research (data not shown).

It is known that metallic nanoparticles can induce an effect known as metal-enhanced fluorescence (MEF), resulting in an enhanced fluorescence of a fluorophore. However, this phenomenon depends strictly on the distance between the analysed particles; MEF typically occurs when the distance is between 5 to 90 nm, but if the distance is lower, the metallic nanoparticle interaction can result in the quenching of the fluorescent signal.[30,31] Hence, our results suggest that daunorubicin is most likely localized in a very close proximity to the platinum nanoparticles, and as such, its fluorescence intensity is reduced upon titration. Similar effects were observed for PtNPs-DOX interactions,[11] another anthracycline agent, and PtNPs-ICR-191 interactions.[10] All these compounds share significant similarities in the chemical structure that include aromatic rings as well as reactive nitrogen residues. Therefore, the mechanism of their interactions with the PtNPs is probably analogous. Moreover, according to literature, other metallic nanoparticles, such as silver or gold also promote such effects,[32–34] therefore we conducted FTIR and NIR analyses to further inspect the nature of the bonding between PtNPs and DAU.

Infrared spectroscopy (IR) is a valuable tool for chemical identification and interpretation of intermolecular interactions.[35] Based on the obtained FTIR spectra we detect either important or interesting physicochemical changes that occur in the sample prepared with sodium citrate solution (Fig. 3).

The most significant spectral changes upon interaction between DAU and PtNPs were observed at 2976 cm^{-1}, corresponding to C–H (CH_2) stretching alkane. In pure DAU this

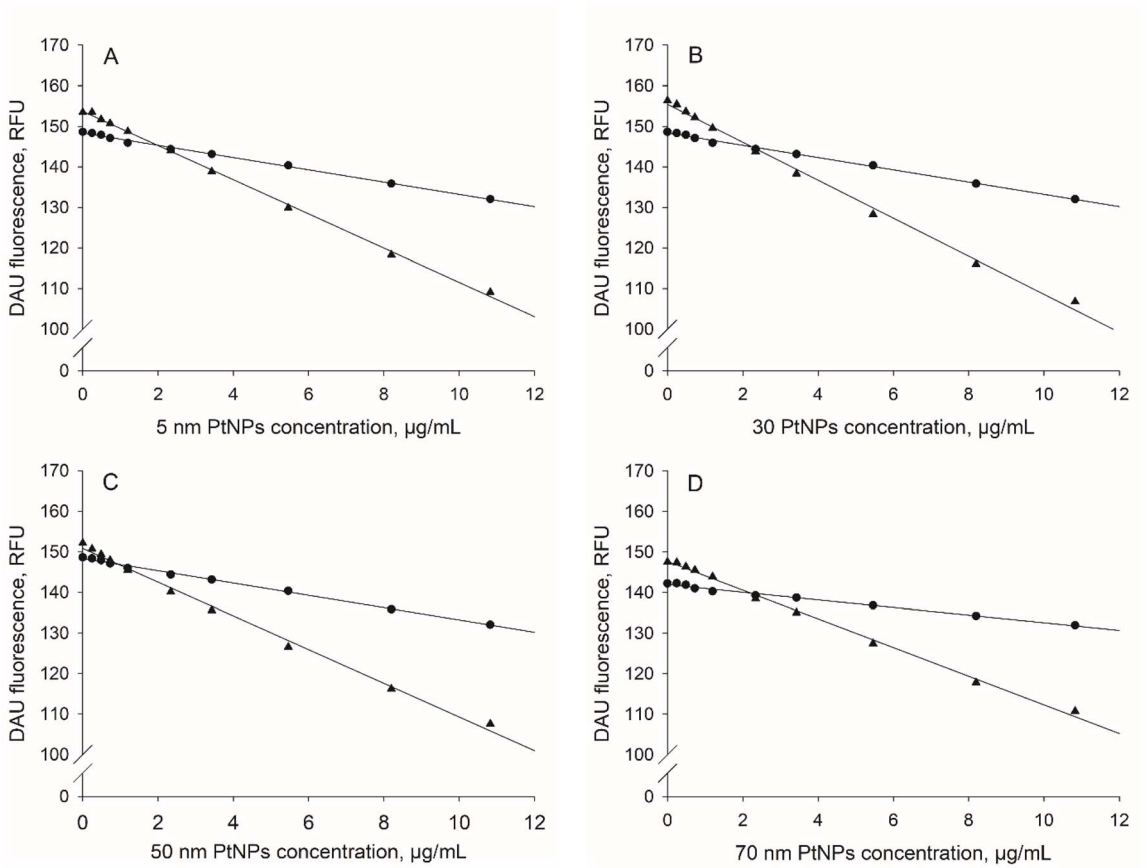

Fig. 2 Fluorescence intensity for platinum nanoparticles (PtNPs) interactions with daunorubicin (DAU) at 590 nm. (A) 5 nm PtNPs, (B) 30 nm PtNPs, (C) 50 nm PtNPs, (D) 70 nm PtNPs; circle – appropriate sodium citrate solution, triangle – platinum nanoparticles. DAU initial concentration 34.7 μM.

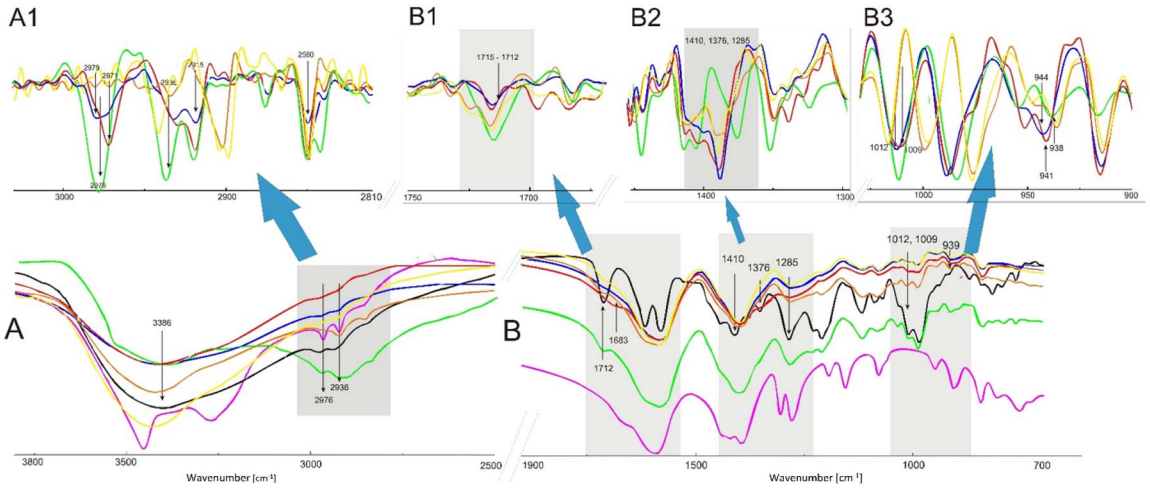

Fig. 3 FTIR spectra of the complexes of daunorubicin (DAU) and platinum nanoparticles (PtNPs) at (A) region 3800–2500 cm^{-1} and at (B) region 1900–700 cm^{-1} and its second derivatives (A1, B1, B2, B3, respectively). 5 nm PtNPs with DAU – blue, 30 nm PtNPs with DAU – orange, 50 nm PtNPs with DAU – red, 70 nm PtNPs with DAU – yellow, sodium citrate – pink, DAU solution in sodium citrate lyophilised – green, DAU alone – black. Arrows indicate the characteristic bands and interactions described in the text. All the samples were lyophilised prior to the experiment.

vibration appears as a single band, but the addition of PtNPs causes a shift to 2965 cm^{-1}, corresponding to decreased energy of this bond. Similarly, O–H stretching region (2930 cm^{-1} to 2840 cm^{-1}) also shifts to lower wavenumbers, suggesting a decrease in energy through interactions between daunorubicin and platinum nanoparticles in all tested sizes.

Significant changes were also recorded for the –C=O asymmetric ketone vibrations (1713 cm^{-1}), which shifted to 1683 cm^{-1}, most notably for 50 nm PtNPs. Another similar effect is observed at the 1088 cm^{-1} and 1070 cm^{-1} area, as the complexes are influenced by nanoparticles and decrease the energy of C–O stretching bond, visible as shift to 1078 cm^{-1} and 1063 cm^{-1}. Surprisingly, the bending alkene C=C substituted, visible as a broad band at 1579 cm^{-1} and in 954–943 cm^{-1} range is also influenced by different sized nanoparticles but there are shifts of bands proving higher energy of this system. Second derivative analysis of spectra was used to better visualize these subtle fluctuations. Complete infrared spectroscopic characterization of DAU and its complexes is shown in Table S1 (SI). Overall, the most prominent interactions were observed for 50 and 70 nm PtNPs-DAU complexes in comparison to the spectrum of sodium citrate solution of DAU, nevertheless 5 and 30 nm PtNPs also induced notable spectral changes, indicating direct interactions with DAU.

Near infrared spectroscopy (NIR) has been found to be advantageous in a wide range of areas in the biotechnological and chemical field, from drug discovery to product development and manufacturing. NIR spectroscopy is sensitive to changes in hydrogen bonding and packing in the crystal lattice, so it can be applied to solid-state analysis, allowing for understanding of molecular interactions.[36] In the near-infrared area mainly vibrations of CH, OH, NH and the SH bonds are observed as overtones or combinations of the fundamental IR bands, resulting in overlapping absorption bands in the spectra.[37] The OH group demonstrates a strong tendency to interact with the chemical neighbourhood, *e.g.*, to form a hydrogen-bond network. The existence of an OH group (as in the DAU compound) is a major spectrum-forming factor in NIR, and therefore many physicochemical influences might be found.[38] Most significant differences in the interaction forces of the PtNPs and DAU were observed in wavenumber region 7000–6300 cm^{-1} as well as near 5176 cm^{-1} which can be assigned to O–H alcohol and free or hydrogen bonded water, respectively[39] (Fig. 4, panel A and B2).

Additional band shifts were observed for O–H/C–O and C–H vibrations, with a change from 4347 cm^{-1} to 4352 cm^{-1} upon PtNPs-DAU complexes formation with 5 nm PtNPs and 70 nm PtNPs. Similar effects were observed at 5176 cm^{-1}, where a shift to lower wavenumbers was recorded for most PtNPs, whereas for 50 nm PtNPs the band shifted upward to 5184 cm^{-1}. The detailed characteristics of NIR analysis are shown in Table S2 (SI). To sum up, these interactions with nanoparticles are responsible for O–H assigned to molecular water or N–H from amine combination bending.

3.3 Endothermic character of DAU-PtNPs interactions

To verify the thermodynamic parameters of PtNPs interactions with DAU, we performed an isothermal titration calorimetry. For 5 nm PtNPs, the registered enthalpy turned out endothermic, with a value of 0.47 ± 0.21 kcal mol^{-1}. The registered total heat increased throughout the remaining 30 nm, 50 nm and 70 nm PtNPs combinations with DAU, yielding in the enthalpy changes of 1.71 ± 0.16 kcal mol^{-1}, 1.89 ± 0.14 kcal mol^{-1}, and 4.36 ± 0.22 kcal mol^{-1}, respectively (Fig. 5). The thermograms are available in the SI (Fig. S1).

The positive values of ITC results, showing that the interactions between PtNPs and DAU are endothermic, can lead to an assumption that the studied interactions are entropy driven processes. Interestingly, the enthalpy increases with the nanoparticles size, as their surface increases and possibly more DAU

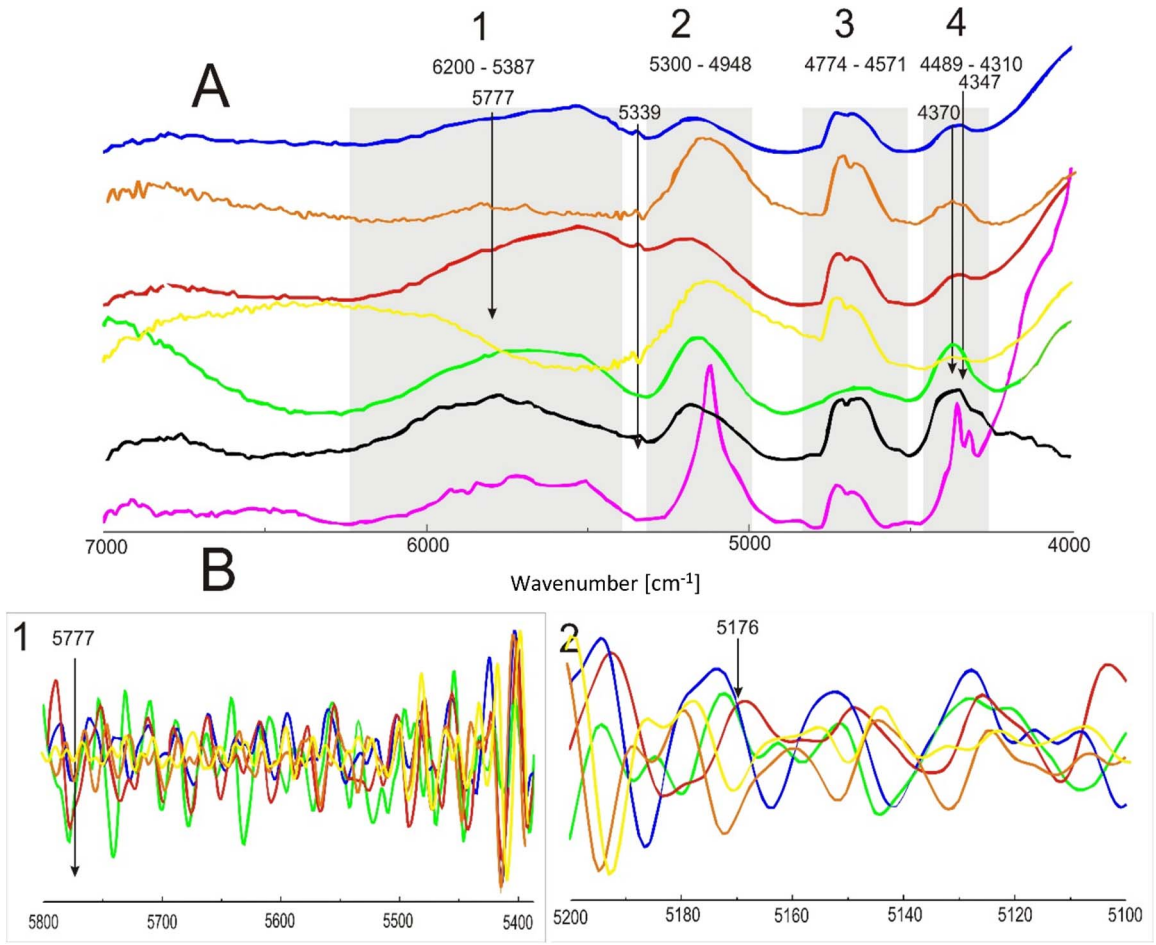

Fig. 4 NIR spectra of the investigated complexes of daunorubicin (DAU) and platinum nanoparticles (PtNPs) (A) in the wavenumber region 7000–4000 cm^{-1} and (B) inlets at regions 6200–5387 cm^{-1} and 5300–4948 cm^{-1}. 5 nm PtNPs with DAU – blue, 30 nm PtNPs with DAU – orange, 50 nm PtNPs with DAU – red, 70 nm PtNPs with DAU – yellow, sodium citrate – pink, DAU alone – black, DAU solution in sodium citrate lyophilised – green. Arrows indicate the characteristic bands and interactions described in the text. All the samples were lyophilised prior to the experiment.

molecules can bind with PtNPs, forming aggregates of various sizes and shapes. Observed effects may be attributed to the changes in the water molecules arrangement around PtNPs during formation of their aggregates with DAU. Namely, the water molecules that form the hydratation shells surrounding PtNPs become reorganized, and the system requires energy to break the hydrogen bonds linking these molecules, resulting in an endothermic outcome. However, this could also be attributed to a change in the molarity of the solvent (from 2 to 4 mM sodium citrate for 70 nm PtNPs). The results available across the literature vary in that matter – for ICR-191 interactions with PtNPs of 75 nm median size the enthalpy was calculated at roughly −4 kcal mol^{-1},[10] whereas for DOX interactions with fullerene C_{60} the values were close to 0 kcal mol^{-1}, with slightly endothermic character.[40] This variability may be attributed to both the type of nanoparticles (metallic or organic) and the solvent in which they are dispersed. Nevertheless, since the results proved direct interactions, further thermal inspection was performed by utilizing differential scanning calorimetry (DSC). The DSC method can be used to characterize thermal transformations of PtNPs and provide insights into the state of a drug in its complexes. Interactions between molecules can influence their chemical structure, hydrophilic properties, and association state, resulting in visible shifts in the thermograms.[41,42] The results of the experiment are shown in Fig. 6.

DSC revealed that both 5 nm and 50 nm PtNPs-DAU complexes demonstrated glass transition (T_g) from the temperature 47.6 to 60 °C, a parameter important for the pharmaceutical industry and observed in nanodispersions or nanocomplexes[43,44] (Fig. 6, part I). On the contrary, pure DAU did not. DSC curves also indicated the presence of water in nanoparticle samples after lyophilization (Fig. 6, part II). The peak at 184.13 °C corresponds to the melting endotherm of DAU (T_m = 208–209 °C). For DAU suspended in sodium citrate sample after lyophilization (Fig. 6, green curve), as well as for DAU complexed with PtNPs at the temperature near 183 °C only a broad area is seen but in the case of 30 nm DAU-PtNPs and 70 nm DAU-PtNPs there is a very small peak, meaning it is a crystalline residual of bulk. Part III of DSC curves of DAU-PtNPs indicates an exothermic process between the temperature range 220–260 °C, corresponding to the decomposition of complexes. Sodium citrate alone exhibited a melting peak at

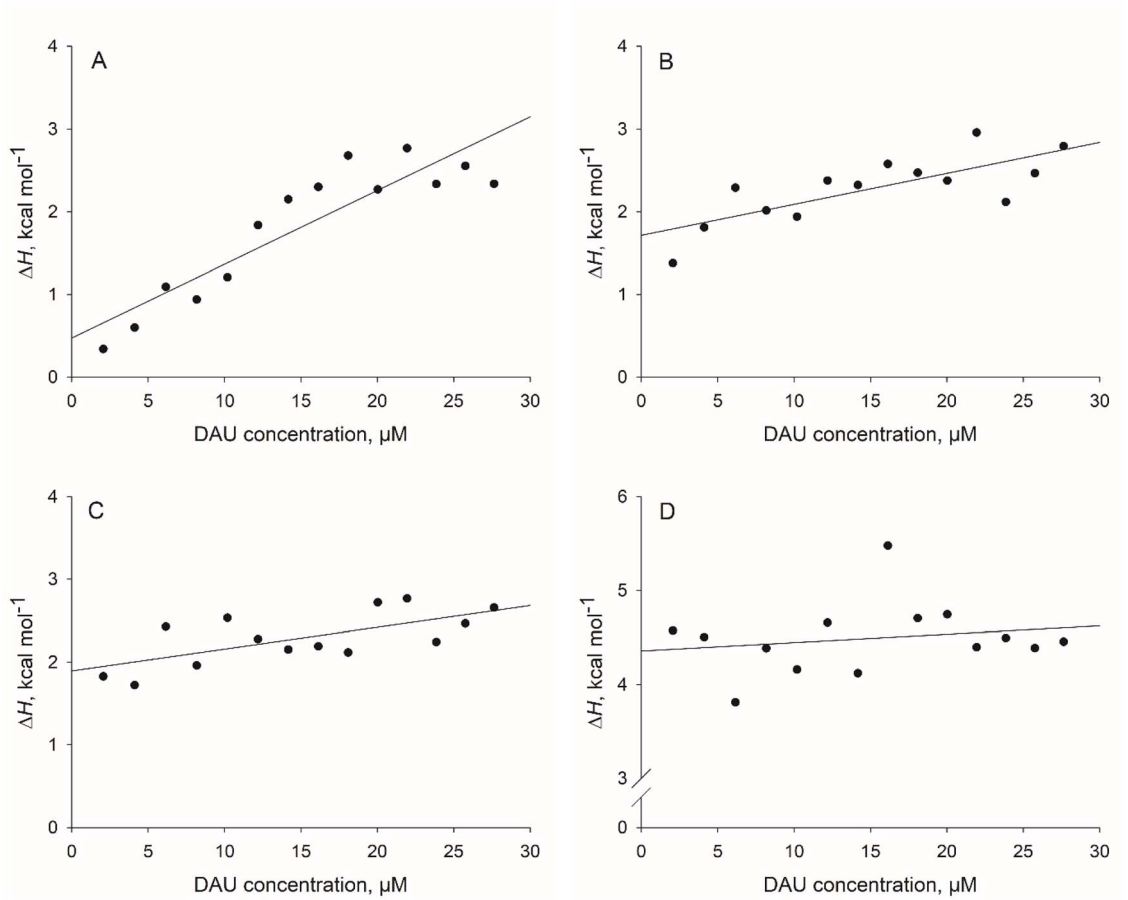

Fig. 5 Isothermal titration calorimetry analysis for the combination of daunorubicin (DAU) with platinum nanoparticles (PtNPs). (A) 5 nm PtNPs ($\Delta H = 0.47 \pm 0.21$ kcal mol^{-1}), (B) 30 nm PtNPs ($\Delta H = 1.71 \pm 0.16$ kcal mol^{-1}), (C) 50 nm PtNPs ($\Delta H = 1.89 \pm 0.14$ kcal mol^{-1}), (D) 70 nm PtNPs ($\Delta H = 4.36 \pm 0.22$ kcal mol^{-1}). DAU concentration range 0.002–0.029 mM, initial PtNPs concentration 0.05 mg mL^{-1}.

164 °C (Fig. 6, pink line) whereas each registered curve for PtNPs showed an exothermic peak at 245 °C (5 nm), 210 °C and 260 °C (30 nm), 230 °C (50 nm) and 250 °C (70 nm). Complexes prepared with 5 nm and 50 nm PtNPs indicate different physicochemical state and thermal properties. We observed an absence of a melting point peak for DAU-loaded nanoparticles at 180 °C for DAU-5 nm PtNPs sample which may be the result of the encapsulation process. A similar situation is known from literature.[45] Differences of DAU-50 nm PtNPs sample's curve at 193 °C may correspond to the change of energy in a complex, but not melting. DAU with 5 nm PtNPs is converted to the amorphous phase as well as the samples with 30 nm and 50 nm PtNPs. It is known that the size of nanoparticles forming complexes has a great effect on their activities.[46] In particular, small particles, such as 5 nm, demonstrate significant activity and stability, however, they have a problem of deactivation. Overall PtNPs influenced thermal properties of DAU in a size-dependent manner.

3.4 Kinetics of DAU release

It is reported that cancer cells have a more acidic pH compared to the healthy cells,[16,17] and that pH targeting can be used for a controlled drug release, leading to the avoidance of harmful effects on healthy tissues. To estimate if the release of daunorubicin can be altered by its interaction with diversely-sized platinum nanoparticles, we performed a release analysis *via* the membrane bag method in three distinct phosphate buffers of pH 5.4, 6.4, and 7.4. The results showed that whereas the drug alone could be released through the membrane pores to 100% in all the tested buffers, this decreased by roughly 30% with the addition of PtNPs in all the tested combinations and buffers (Fig. 7). The statistical analysis is available in SI (Tables S3–S6).

The most significant difference in the maximum released level was observed for 30 nm PtNPs at pH 5.4. On the contrary, 70 nm PtNPs exhibited the lowest degree of variation in terms of changing the diffusion level of DAU, irrespective of the buffer's pH. DAU itself showed a release to 100% in all the tested buffers within the first 12 h of the experiments. However, the addition of PtNPs leads to a decrease in the maximum diffusion, most notably in the case of 30 nm PtNPs. What is more, the mean release percentage was the lowest at pH 7.4 (75%), and the highest at pH 6.4 (85%). This observation is somewhat consistent with other studies, where the diffusion of anthracyclines was altered by various metallic nanoparticles, and resulted in a significantly higher drug release at lower pH.[47–49] Interestingly,

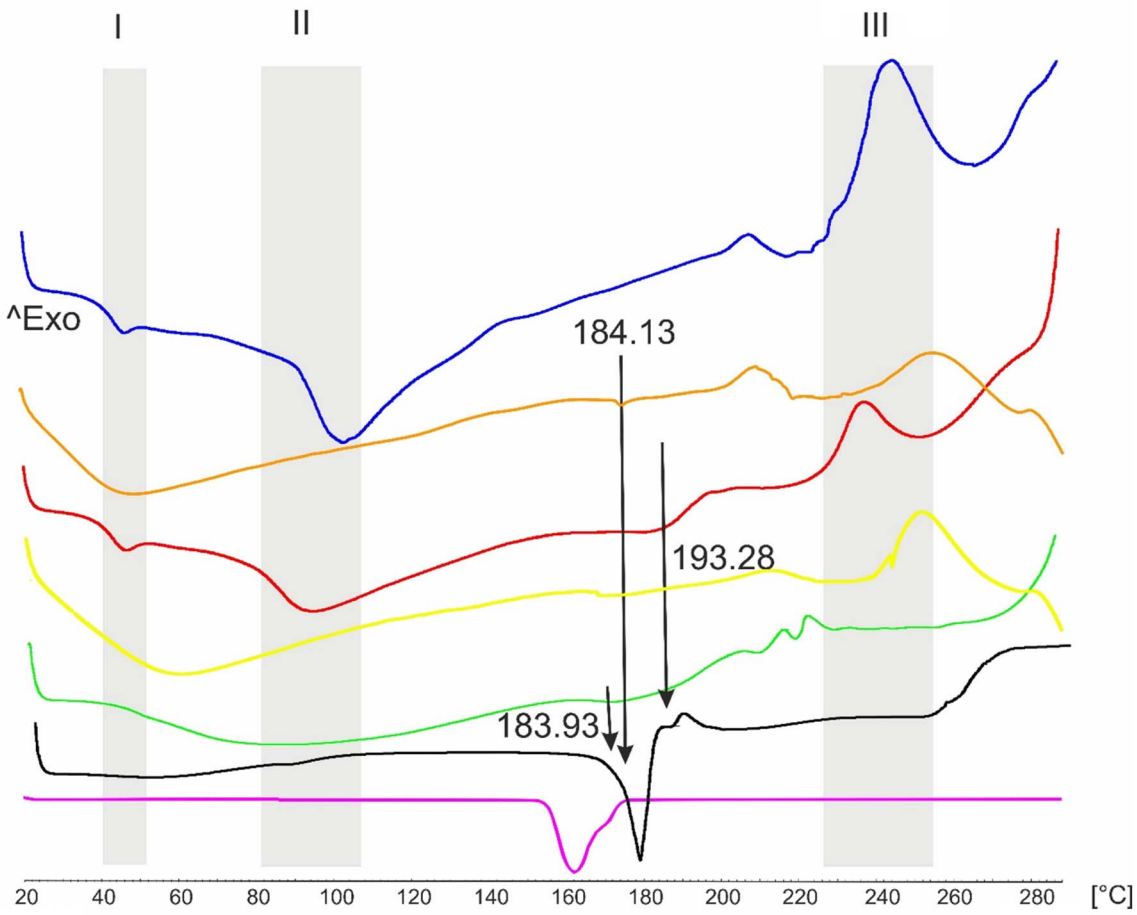

Fig. 6 DSC curves of daunorubicin (DAU) mixtures with platinum nanoparticles (PtNPs). 5 nm PtNPs with DAU – blue, 30 nm PtNPs with DAU – orange, 50 nm PtNPs with DAU – red, 70 nm PtNPs with DAU – yellow, DAU solution in sodium citrate lyophilised – green, DAU alone – black, sodium citrate – pink.

in all the buffers combination, 70 nm PtNPs with DAU yielded the highest drug diffusion in comparison to the remaining tested PtNPs sizes. This dissimilarity could be attributed to a smaller surface area to volume ratio, resulting in less possible interactions between the nanoparticles and the drug. Overall, the lowered release of DAU when combined with PtNPs is correlated with the results of DLS and NTA, where we observed the formation of PtNPs-DAU aggregates. Moreover, FTIR and NIR confirmed the interactions with most likely through formation of hydrogen, as well as electrostatic bonds between the nanoparticles and the drug. We conclude that combining PtNPs with DAU significantly alters anthracycline's release profiles irrespective of the pH.

Furthermore, we analysed the data utilizing the Korsmeyer–Peppas and Hopfenberg models, and calculated the maximum of the released substance (Q_∞), the exponent n, which is used to determine the transport mechanism, and the relaxation rate of this process (k_{KP} and k_r) – Table 3. The relaxation rate k_{KP}, based on the Korsmeyer–Peppas model, is related to Fick-type diffusion,[50] while the relaxation rate k_r comes from the Hopfenberg model.[51]

These models are commonly used to analyse drug release from polymer matrices. In the case of dialysis bags, the diffusion process can typically be described by the Fickian equation. However, in this instance, DAU release proceeded similarly to the aforementioned case of polymer matrices. Based on these models, we established that the release exponents indicated the presence of anomalous transport within all the experiments, with n values being in the range $0.5 < n < 1$. This implies that in all the samples, in addition to Fickian diffusion, there is an additional process influencing the release mechanism. Assuming that the DAU-nanoparticle system aggregates, and that this aggregation is mediated by hydrogen bonds, it may erode, similar to some polymer matrices, resulting in nonlinear DAU release.[52] The similar release rate values obtained from the fitting result from the fact that, as previously reported, aggregates vary in size, and therefore the obtained result is an average. In literature, the results are incoherent in that matter, as the n exponent is sometimes reported to be below 0.5, suggesting a semi-fickian diffusion, other times it falls in the range $0.5 < n < 1$, similarly to our study.[49,53–55] Nevertheless, it is visible that platinum nanoparticles alter the rate at which daunorubicin is released, however, the change seems to be unaffected by the pH of the buffer.

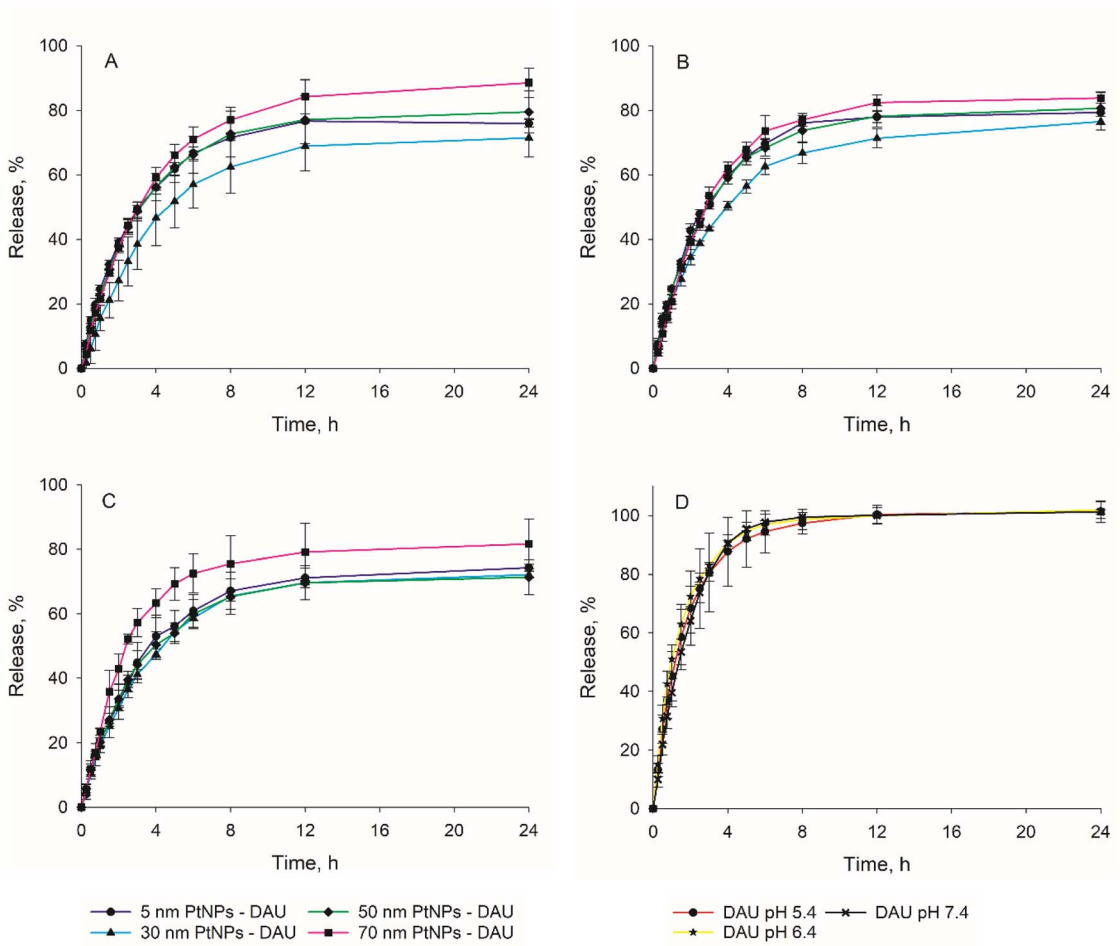

Fig. 7 Analysis of daunorubicin (DAU) release from DAU-platinum nanoparticles (PtNPs) complexes at various pH. (A) pH 5.4, (B) pH 6.4, (C) pH 7.4, (D) DAU alone.

Table 3 Korsmeyer–Peppas and Hopfenberg modelling analysis

	5 nm			30 nm			50 nm			70 nm			DAU alone		
pH	5.4	6.4	7.4	5.4	6.4	7.4	5.4	6.4	7.4	5.4	6.4	7.4	5.4	6.4	7.4
Q_∞ (%)	76.5	79.1	75.1	73	76.7	72.7	79.3	80	69.5	83.8	86.1	82.5	99.3	99.7	103
k_r	0.35	0.34	0.31	0.24	0.28	0.28	0.32	0.34	0.3	0.27	0.3	0.33	0.58	0.66	0.5
k_{KP}	23.9	23.8	20.7	14	21.1	18.2	22.5	23.6	18.6	19.3	20	21.3	44.1	49.1	36
n	0.69	0.69	0.73	0.94	0.67	0.75	0.72	0.73	0.76	0.82	0.87	0.91	0.74	0.70	0.78
R^2	0.99	0.99	0.99	0.99	0.99	0.99	0.99	0.99	0.99	0.99	0.99	0.99	0.99	0.99	0.99

3.5 PtNPs influence DAU's biological activity

Taking into consideration the results of physicochemical analysis, we performed Ames mutagenicity tests on *Salmonella enterica* serovar Typhimurium TA98 strain to investigate the effects of PtNPs-DAU interactions on the DAU's mutagenic potential. 5 nm PtNPs significantly lowered the mutagenic effect in all tested concentrations (Fig. 8A). For the remaining sizes, we observed similar effects, excluding the lowest concentration of PtNPs (Fig. 8B–D). The optimal concentration of DAU was chosen prior to the experiment (SI, Fig. S2). Importantly, PtNPs alone did not exhibit any mutagenic effects (SI, Fig. S3).

The Ames mutagenicity assay is a valuable tool for a moderately fast screening of the effects that interactions between two compounds have on the biological effects of one of them.[56] Our results show that with increasing concentrations of PtNPs the mutagenicity of DAU is lowered. Similar results were observed for PtNPs-DOX interactions,[11] as well as for PtNPs-ICR-191.[10] This could be attributed to aforementioned formation of PtNPs-

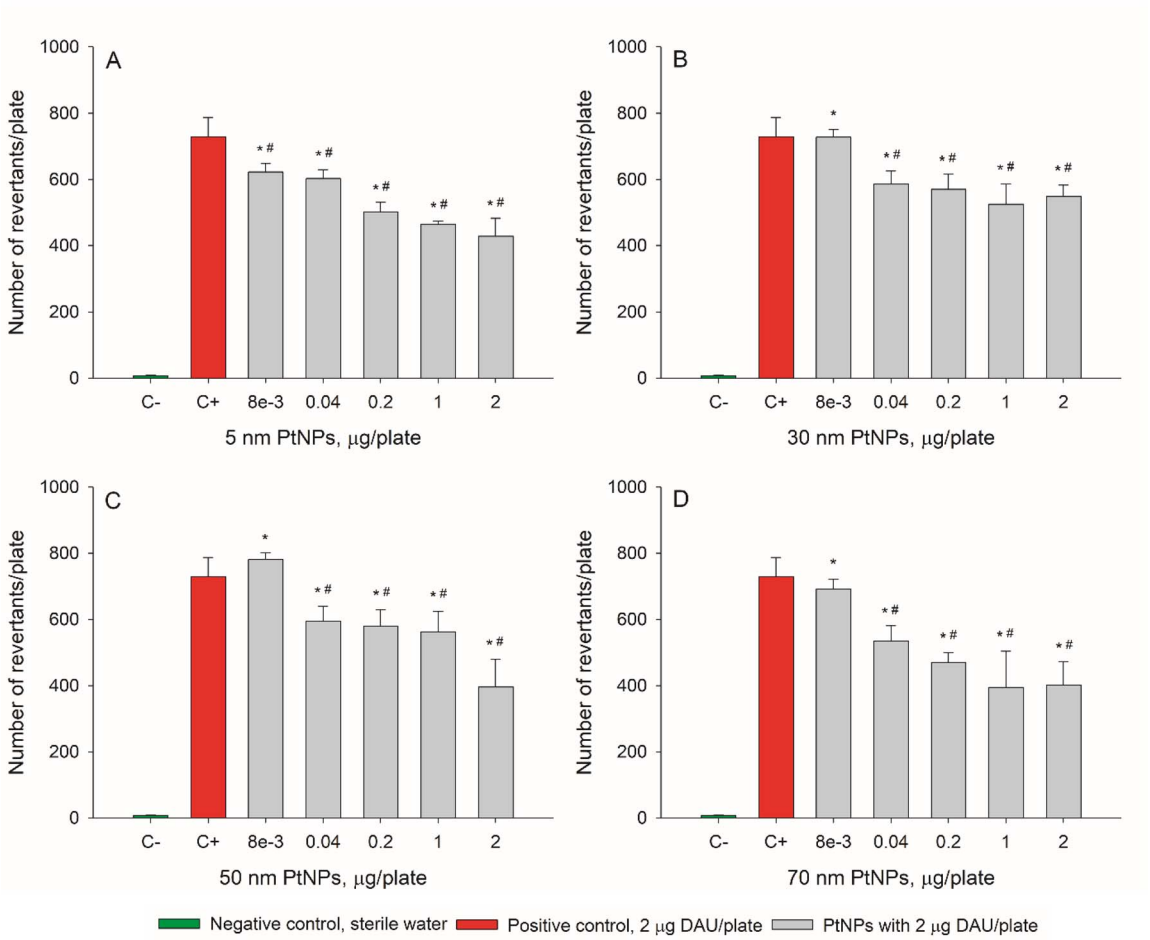

Fig. 8 Influence of platinum nanoparticles (PtNPs) on the mutagenicity of daunorubicin (DAU) in *Salmonella enterica* serovar Typhimurium TA98 strain. (A) 5 nm PtNPs with DAU, (B) 30 nm PtNPs with DAU, (C) 50 nm PtNPs with DAU, (D) 70 nm PtNPs with DAU. C− negative control (green, sterile water), C+ positive control (red, 2 μg DAU/plate). Results are reported as the average number of revertants per plate ± SD. *- significant difference from the negative control ($p < \alpha$; $\alpha = 0.05$); # – significant difference from the positive control ($p < \alpha$; $\alpha = 0.05$).

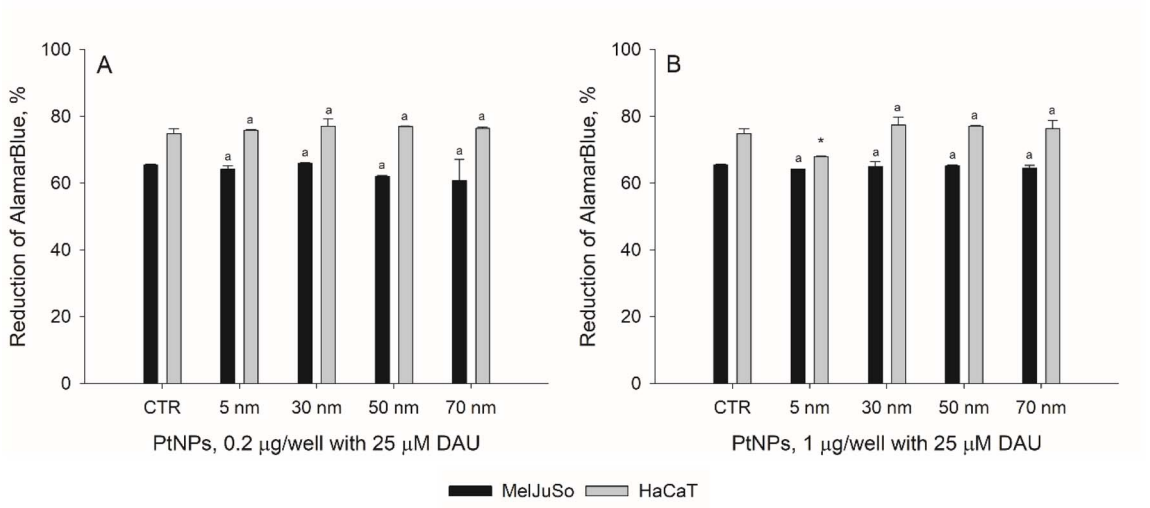

Fig. 9 Influence of platinum nanoparticles (PtNPs) on the cytotoxicity of daunorubicin (DAU) in MelJuSo and HaCaT cell lines. (A) 0.2 μg of PtNPs/well with 25 μM DAU, (B) 1 μg of PtNPs/well with 25 μM DAU. CTR – control (25 μM DAU), PtNPs-DAU mixtures in given concentrations with constant 25 μM DAU. MelJuSo cell line – black, HaCaT cell line – grey. Results are reported as the mean percentage difference between treated cells and untreated control ± SD. a-no significant difference from the control with DAU within a single cell line ($p < \alpha$; $\alpha = 0.05$), *- significant difference from the control with DAU within a single cell line ($p < \alpha$; $\alpha = 0.05$).

DAU aggregates, making the drug unavailable for the cells to incorporate. With the increasing concentration of PtNPs, the aggregates most likely become greater in size and bind more molecules of DAU, leaving it less available for the cells, thus resulting in lower mutagenicity.

Next, we analysed the influence of PtNPs on DAU's cytotoxicity on two eukaryotic cell lines: non-cancerous HaCaT and cancerous MelJuSo. Prior to testing various combinations, we examined PtNPs and observed they did not significantly alter the growth of neither cell lines (SI, Fig. S4). Based on the effects of PtNPs concentrations with Ames test, we examined their cytotoxicity at 0.2 and 1 μg per well with addition of 25 μM DAU (Fig. 9). None of the investigated combinations altered the cytotoxicity of the drug, apart from 5 nm at 1 μg per well in HaCaT cell line (Fig. 9B).

Despite various reports in the literature regarding PtNPs and their cytotoxic effects towards cancer cells, we did not observe any significant changes in cells viability in our tests. What is interesting, PtNPs significantly enhanced ICR-191 toxicity towards MelJuSo cells with no harmful effects towards healthy HaCaT cells.[10] Moreover, PtNPs significantly influenced cytotoxicity of DOX, one of 4 anthracyclines, with the MelJuSo cells being either killed in a similar or intensified manner, than with drug alone, while simultaneously enhancing the viability of HaCaT cells.[11] The dissimilarity between the observed effects of these two anthracyclines and their combination with PtNPs may be attributed to the conformational change at C-14; DOX has an –H, while DAU has –OH group. It may seem a minor change, but it could alter the activity profile of the drug, as well as its binding capability (*i.e.* stability of formed aggregates), resulting in lesser effects towards these cell lines. It's worth noting that the observed effects can vary depending on chosen cell lines. Nevertheless, the results conclude that there are no significant effects of PtNPs-DAU interactions on the cytotoxicity of the drug in HaCaT and MelJuSo cell lines at the examined concentrations.

4 Conclusions

In summary, platinum nanoparticles (PtNPs) of distinct sizes 5, 30, 50 and 70 nm have been shown to interact with daunorubicin (DAU), leading to the formation of aggregates. Significant quenching of fluorescence indicated direct interaction between DAU and PtNPs of all sizes, while FTIR and NIR confirmed that providing precise data for exact bonds within the chemical structure of DAU. Calorimetric analyses using ITC and DSC techniques provided additional information on the interactions studied and showed that the interactions are of an endothermic nature, driven by entropy. Combining PtNPs with DAU results in altered DAU release kinetics, most notably by 30 nm PtNPs. The observed interactions reduce DAU's mutagenic capabilities in *Salmonella enterica* serovar Typhimurium TA98 strain, however, no significant effects were observed in neither cancerous MelJuSo nor non-cancerous HaCaT cell lines. Our study provides a thorough examination of PtNPs-DAU interactions and their influence on the drug's activity, and warrants further eukaryotic studies in regards to PtNPs role as potential activity modulators of classical anticancer drugs.

Author contributions

Marcin Zakrzewski: investigation, formal analysis, visualization, validation, writing – original draft. Patrycja Bełdzińska: methodology, investigation, writing – review & editing. Felicja Gajdowska – investigation. Grzegorz Gołuński: writing – review & editing, methodology, visualization. Karolina Gackowska: investigation, writing – review & editing. Justyna Strankowska: investigation, writing – review & editing. Marzena Jamrógiewicz: resources, investigation, writing – review & editing. Dariusz Wyrzykowski: resources, investigation, writing – review & editing. Katarzyna Grzyb: investigation, writing – review & editing. Danuta Gutowska-Owsiak: resources, writing – review & editing. Anna Synak: resources, investigation. Piotr Bojarski: resources. Jacek Piosik: conceptualization, project administration, resources, supervision, writing – review & editing.

Conflicts of interest

There are no conflicts to declare.

Data availability

The data of this study are available from the corresponding author upon request.

Supplementary information is available. See DOI: **https://doi.org/10.1039/d5ra02827b**.

Acknowledgements

The NTA equipment was purchased within the POIR.04.04.00-00-21FA/16-00 project, carried out within the First TEAM program of the Foundation for Polish Science, co-financed by the European Union under the European Regional Development Fund (awarded to DGO).

References

1 F. Bray, M. Laversanne, S. Hyuna, J. Ferlay, R. L. Siegel, I. Soerjomataram and J. D. Ahmedin, *Ca – Cancer J. Clin.*, 2024, **74**, 229–263.
2 T. Olivier, A. Haslam and V. Prasad, *JAMA Netw. Open*, 2021, **4**, E2138793.
3 B. E. Wilson, S. Jacob, M. L. Yap, J. Ferlay, F. Bray and M. B. Barton, *Lancet Oncol.*, 2019, **20**, 769–780.
4 X. Mao, S. Wu, D. Huang and C. Li, *Acta Pharm. Sin. B*, 2024, **14**, 2901–2926.
5 I. Khan, K. Saeed and I. Khan, *Arab. J. Chem.*, 2019, **12**, 908–931.
6 M. Jeyaraj, S. Gurunathan, M. Qasim, M. H. Kang and J. H. Kim, *Nanomaterials*, 2019, **9**, 1719.
7 A. Abed, M. Derakhshan, M. Karimi, M. Shirazinia, M. Mahjoubin-Tehran, M. Homayonfal, M. R. Hamblin, S. A. Mirzaei, H. Soleimanpour, S. Dehghani, F. F. Dehkordi and H. Mirzaei, *Front. Pharmacol*, 2022, **13**, 797804.

8 V. Borse, A. Kaler and U. C. Banerjee, *Int. J. Electr. Electron. Res.*, 2015, **11**, 2320–9569.
9 M. Kutwin, E. Sawosz, S. Jaworski, M. Hinzmann, M. Wierzbicki, A. Hotowy, M. Grodzik, A. Winnicka and A. Chwalibog, *Arch. Med. Sci.*, 2017, **13**, 1322–1334.
10 A. Borowik, R. Banasiuk, N. Derewonko, M. Rychlowski, M. Krychowiak-Masnicka, D. Wyrzykowski, M. Ziabka, A. Woziwodzka, A. Krolicka and J. Piosik, *Sci. Rep.*, 2019, **9**, 1–11.
11 P. Bełdzińska, B. Galikowska-Bogut, M. Zakrzewski, K. Bury, M. Jamrógiewicz, D. Wyrzykowski, G. Gołuński, R. Sądej and J. Piosik, *Chem. Biol. Interact.*, 2025, **407**, 111365.
12 P. V. Asharani, N. Xinyi, M. P. Hande and S. Valiyaveettil, *Nanomedicine*, 2010, **5**, 51–64.
13 A. Watanabe, M. Kajita, J. Kim, A. Kanayama, K. Takahashi, T. Mashino and Y. Miyamoto, *Nanotechnology*, 2019, **20**, 455015.
14 S. Gurunathan, M. Jeyaraj, M. H. Kang and J. H. Kim, *Int. J. Mol. Sci.*, 2020, **21**, 6792.
15 S. Gurunathan, M. Jeyaraj, M. H. Kang and J. H. Kim, *Nanomaterials*, 2019, **9**, 1089.
16 M. C. Brahimi-Horn and J. Pouysségur, *FEBS Lett.*, 2007, **581**, 3582–3591.
17 P. Vaupel, *Semin. Radiat. Oncol.*, 2004, **14**, 198–206.
18 B. Fu, M. Dang, J. Tao, Y. Li and Y. Tang, *J. Colloid Interface Sci.*, 2020, **570**, 197–204.
19 S. Mukherjee, R. Kotcherlakota, S. Haque, D. Bhattacharya, J. M. Kumar, S. Chakravarty and C. R. Patra, *Mater. Sci. Eng. C*, 2020, **108**, 110375.
20 B. Pudhuvai, K. Beneš, V. Čurn, A. Bohata, J. Lencova, R. Vrzalova, J. Barta and V. Matha, *Microorganisms*, 2024, **12**, 2639.
21 M. B. Martins-Teixeira and I. Carvalho, *ChemMedChem*, 2020, **15**, 933–948.
22 J. V. McGowan, R. Chung, A. Maulik, I. Piotrowska, J. M. Walker and D. M. Yellon, *Cardiovasc. Drugs Ther.*, 2017, **31**, 63.
23 R. Mattioli, A. Ilari, B. Colotti, L. Mosca, F. Fazi and G. Colotti, *Mol. Aspects Med.*, 2023, **93**, 101205.
24 D. D. Perrin and B. Dempsey, *Buffers for pH and Metal Ion Control*, DOI: 10.1007/978-94-009-5874-6.
25 A. Woziwodzka, A. Gwizdek-Wiśniewska and J. Piosik, *Bioorg. Chem.*, 2011, **39**, 10–17.
26 G. Gołuński, K. Konkel, B. Galikowska Bogut, P. Bełdzińska, K. Bury, M. Zakrzewski, K. Butowska, R. Sądej and J. Piosik, *Sci. Rep.*, 2024, **14**, 18544.
27 K. Butowska, W. Kozak, M. Zdrowowicz, S. Makurat, M. Rychłowski, A. Hać, A. Herman-Antosiewicz, J. Piosik and J. Rak, *Struct. Chem.*, 2019, **30**, 2327–2338.
28 M. Gumustas, C. T. Sengel-Turk, A. Gumustas, S. A. Ozkan and B. Uslu, *Multifunct. Syst. Comb. Delivery, Biosens. Diagn.*, 2017, 67–108.
29 X. Tian, M. R. Nejadnik, D. Baunsgaard, A. Henriksen, C. Rischel and W. Jiskoot, *J. Pharm. Sci.*, 2016, **105**, 3366–3375.
30 S. Lee and S. H. Kang, *Biosensors*, 2023, **13**, 376.
31 Y. Jeong, Y. M. Kook, K. Lee and W. G. Koh, *Biosens. Bioelectron.*, 2018, **111**, 102–116.
32 J. Zhu, J. jun Li, A. qing Wang, Y. Chen and J. wu Zhao, *Nanoscale Res. Lett.*, 2010, **5**, 1496–1501.
33 A. A. Aboalhassan, S. A. El-Daly, E. Z. M. Ebeid and M. A. S. Sakr, *J. Fluoresc.*, 2022, **32**, 2257–2269.
34 A. Farokhcheh and N. Alizadeh, *J. Iran. Chem. Soc.*, 2013, **10**, 799–805.
35 Á. I. López-Lorente and B. Mizaikoff, *Trac. Trends Anal. Chem.*, 2016, **84**, 97–106.
36 E. Räsänen and N. Sandler, *J. Pharm. Pharmacol.*, 2007, **59**, 147–159.
37 E. W. Ciurczak and J. K. Drennen III, *Pharmaceutical and Medical Applications of Near-Infrared Spectroscopy*, DOI: 10.1201/9780203910153.
38 M. A. Czarnecki, Y. Morisawa, Y. Futami and Y. Ozaki, *Chem. Rev.*, 2015, **115**, 9707–9744.
39 H. Maeda, Y. Ozaki, M. Tanaka, N. Hayashi and T. Kojima, *J. Near Infrared Spectrosc.*, 1995, **3**, 191–201.
40 Y. I. Prylutskyy, M. P. Evstigneev, I. S. Pashkova, D. Wyrzykowski, A. Woziwodzka, G. Gołuński, J. Piosik, V. V Cherepanov and U. Ritter, *Phys. Chem. Chem. Phys.*, 2316, **16**, 23164.
41 O. Borges, G. Borchard, J. C. Verhoef, A. De Sousa and H. E. Junginger, *Int. J. Pharm.*, 2005, **299**, 155–166.
42 A. C. Y. Wong and F. Lam, *Polym. Test.*, 2002, **21**, 691–696.
43 D. J. Van Drooge, W. L. J. Hinrichs, M. R. Visser and H. W. Frijlink, *Int. J. Pharm.*, 2006, **310**, 220–229.
44 N. Jadhav, V. L. Gaikwad, K. J. Nair and H. Kadam, *Asian J. Pharm.*, 2009, **3**, 82–89.
45 E. Nikolskaya, M. Sokol, M. Faustova, O. Zhunina, M. Mollaev, N. Yabbarov, O. Tereshchenko, R. Popov and E. Severin, *Acta Bioeng. Biomech.*, 2018, **20**, 65–77.
46 H. Inokawa, T. Ichikawa and H. Miyaoka, *Appl. Catal., A*, 2015, **491**, 184–188.
47 H. Zhang, C. Wang, B. Chen and X. Wang, *Int. J. Nanomed.*, 2012, **7**, 235–242.
48 J. Nogueira, S. F. Soares, C. O. Amorim, J. S. Amaral, C. Silva, F. Martel, T. Trindade and A. L. Daniel-Da-Silva, *Molecules*, 2020, **25**, 333.
49 Q. Yang, J. Peng, Y. Xiao, W. Li, L. Tan, X. Xu and Z. Qian, *ACS Appl. Mater. Interfaces*, 2018, **10**, 150–164.
50 S. C. Basak, B. M. J. Reddy and K. P. L. Mani, *Indian J. Pharm. Sci.*, 2006, **68**, 594–598.
51 M. Miotke-Wasilczyk, M. Józefowicz, J. Strankowska and J. Kwela, *Materials*, 2021, **14**, 1842.
52 J. Siepmann and F. Siepmann, *J. Controlled Release*, 2012, **161**, 351–362.
53 J. L. Sánchez-Orozco, H. I. Meléndez-Ortiz, B. A. Puente-Urbina, O. S. Rodríguez-Fernández, A. Martínez-Luévanos and L. A. García-Cerda, *Polymers*, 2023, **15**, 968.
54 P. Rananaware, P. Pandit and V. Brahmkhatri, *Discover Nano*, 2024, **19**, 201.
55 Y. Gao, J. Zuo, N. Bou-Chacra, T. D. J. A. Pinto, S. D. Clas, R. B. Walker and R. Löbenberg, *BioMed Res. Int.*, 2013, **2013**, 136590.
56 A. Woziwodzka, G. Gołuński and J. Piosik, *ISRN Biophys.*, 2013, **2013**, 1–11.